



# New postcranial remains from the Lealt Shale Formation of the Isle of Skye, Scotland, showcase hidden pterosaur diversity in the Middle Jurassic

Natalia Jagielska<sup>1,2\*</sup>, Thomas J. Challands<sup>1</sup>, Michael O’Sullivan<sup>3</sup>, Dugald A. Ross<sup>4</sup>, Nicholas C. Fraser<sup>1,2</sup>, Mark Wilkinson<sup>1</sup> and Stephen L. Brusatte<sup>1,2</sup>

<sup>1</sup> School of Geosciences, University of Edinburgh, Grant Institute, The King’s Buildings, James Hutton Road, Edinburgh EH9 3FE, UK

<sup>2</sup> National Museums Scotland, Chambers St, Edinburgh EH1 1JF, UK

<sup>3</sup> Unaffiliated, Limerick, Ireland

<sup>4</sup> Staffin Museum, Ellishadder, Staffin IV51 9JE, UK

NJ, 0000-0001-7602-5878

\* Correspondence: [N.Jagielska@sms.ed.ac.uk](mailto:N.Jagielska@sms.ed.ac.uk)

**Abstract:** The Early to Middle Jurassic transition was significant in pterosaur evolution, during which these volant reptiles exploded in diversity alongside dinosaurs and other animals. It has long been thought, however, that pterosaurs did not develop large wingspans until after the Jurassic, a notion challenged by the recent discovery of *Dearc sgiathanach* in the Bathonian-aged Lealt Shale Formation of the Isle of Skye, Scotland, whose holotype specimen had an estimated wingspan greater than 2.5 m. We here report the discovery of a new pterosaur specimen from the Lealt Shale Formation, comprising a tibiotarsus, metatarsal, pedal phalanges and caudal vertebrae. The elongate tail vertebrae with ossified processes indicate that the specimen is a non-pterodactyloid pterosaur, albeit its fragmentary nature makes it difficult to determine whether it belongs to a new taxon. Its metatarsal and caudal vertebrae are considerably larger than corresponding bones in the *Dearc* holotype, indicating that it belonged to an even larger individual, thus demonstrating that pterosaurs with broad wingspans were not anomalous in the Middle Jurassic. The growing Middle Jurassic pterosaur record of Scotland and England, although mostly represented by isolated and fragmentary fossils, reveals a high diversity of clades, long obscured by the lack of well-preserved skeletons.

Received 30 January 2023; revised 4 April 2023; accepted 14 April 2023

Pterosaurs are a specialized group of reptiles that were capable of active flight (Witton 2013). Their fossil record begins in the Late Triassic (Dalla Vecchia 2013; Upchurch *et al.* 2015) and by the Late Jurassic reaches global distribution (Alocón-Muñoz *et al.* 2021) in habitats ranging from arid deserts (Britt *et al.* 2018) to sub-tropical lagoons (Bennett 1996) and forests (Zhou *et al.* 2021). Select genera of pterosaurs are known from tens of well-preserved skeletons (Beardmore *et al.* 2017), such as *Rhamphorhynchus*, *Pterodactylus* (Bennett 1995, 1996) and *Dorygnathus* (Padian 2008). Species with such an abundant fossil record are rare, however, and restricted to select periods and lagerstätte locations (Dean *et al.* 2016), whereas most species of pterosaurs are known from a single, partial holotype. This creates gaps in our understanding of the evolution of these animals, particularly concerning the origin of large wingspans and body size in pterosaurs, the Jurassic–Cretaceous extinction of early branching non-pterodactyloids and the diversification of late branching pterodactyloids in the Cretaceous. Although marine and lagoonal environments of the Early and Late Jurassic have yielded a variety of high-quality pterosaur fossils, with dubious dating of Chinese deposits (Sullivan *et al.* 2014), this is currently not the case for the Middle Jurassic, a period associated with the mass diversification of many tetrapod groups (Jagielska *et al.* 2022) such as mammals (Close *et al.*

2015), dinosaurs (Benson 2018) and amphibians (Jones *et al.* 2022) among others, leading to all novel material from this time interval being of importance.

Recently, the Lealt Shale Formation (Bathonian) of the Isle of Skye, Scotland, yielded one of the world’s best-preserved Middle Jurassic pterosaur fossils: an articulated and well-preserved skeleton established as the holotype of a new species of non-pterodactyloid pterosaur, *Dearc sgiathanach* (Jagielska *et al.* 2022). With an estimated wingspan greater than 2.5 m, this skeleton has one of the largest wingspans of any Jurassic pterosaur globally and indicates that pterosaurs achieved large body sizes earlier in their evolution than previously recognized (Jagielska *et al.* 2022). The description of *Dearc* prompted a re-examination of many highly fragmentary fossils from the Middle Jurassic of England, some of which also were suggestive of larger pterosaurs, with wingspans perhaps approaching 4 m (Jagielska *et al.* 2022). Still, other than the *D. sgiathanach* holotype, these records of Middle Jurassic pterosaurs are meagre, meaning that any new discoveries are instrumental in testing the idea that large pterosaurs were common during this time interval.

During the same 2017 field season in which the *Dearc* holotype was discovered, one of us (TJC) recovered additional 3D pterosaur bones nearby, in rocks of the Lealt Shale Formation at Brothers’ Point on the Trotternish

Peninsula of Skye, comprising a partial hind limb (a tibia with pedal elements) and middle caudal vertebrae. The specimen is moderately well preserved, and we here show that, like the *Dearc* holotype, it represents a large non-pterodactyloid pterosaur.

### Geological background

The major Middle Jurassic stratigraphic units in Britain that are known to host pterosaur fossils include the Great Oolite Group in southern England and the Great Estuarine Group in Hebridean Scotland, which were formed in a largely coeval (*Zigzagiceras zigzag* ammonite biozone to *Procerites pogracilis* ammonite biozone) shallow seaway (Harris and Hudson 1980; Barron *et al.* 2012). The lithologies vary from marine carbonates and muds in the south and diversify to include deposits of terrestrial affinities (fluvial, deltaic and marginal marine) in the north (Hesselbo *et al.* 2003; Barron *et al.* 2012). Deposition occurred in an extensional rift basin associated with the break-up of Pangaea, forming a shallow seaway connecting the Boreal Sea with the Tethys Ocean, eventually opening into the ‘Viking corridor’ (Korte *et al.* 2015). The seaway was dotted with a series of small landmasses on platforms fluctuating in relief. In the Middle Jurassic, subsidence and deposition counteracted each other, allowing for the formation of a thick shallow-marine sequence comprising carbonate facies with occasional input of terrigenous material. The non-marine nature of some of the deposits provides an insufficient amount of index fossils, which complicates the accurate dating of such individual units (Barron *et al.* 2012).

The British Middle Jurassic is known to preserve vertebrate fossil remains, including pterosaurs (O’Sullivan and Martill 2018). The Bathonian Oxfordshire sediments of the Great Oolite Group capture the fauna and flora of terrestrial, nearshore fluvial, deltaic and open-marine realms, giving a breadth of represented environments (Fraser and Sues 1997). In Scotland, the Great Estuarine Group (Harris and Hudson 1980) encompasses a laterally continuous sequence from Upper Bajocian to Lower Callovian across the Hebrides. Notable pterosaur remains from the Great Estuarine sequence have recently been recovered from the Kilmaluag Formation, formed in mudflats and lagoons, including dentary fragments (Barrett *et al.* 2008), postcranial material (fig. 8d of Panciroli *et al.* 2020), and a more complete associated partial skeleton described in a preprint (Martin-Silverstone *et al.* 2022). The holotype skeleton of *Dearc* was discovered in another unit, the Lonfean Member of the Lealt Shale Formation, deposited in lagoons on a marginal-marine platform (Harris and Hudson 1980; Hudson and Wakefield 2018). These Lealt Shale deposits are fossiliferous, known mostly for numerous dinosaur tracksites (dePolo 2018).

### Systematic palaeontology

*Specimen.* NMS G.2023.1.1 consists of bones preserved in three dimensions, with localized crushing and moderate disarticulation. The bones preserved include a caudal vertebral section, tibia and pedal elements. The presence of elongate caudal vertebra with bony filiform and interlocking zygapophyses identifies the fossil as a sizeable (comparable

with *Dearc* with wingspan comparable to 2 m) pterosaur of derived non-pterodactyloid grade (Lü *et al.* 2010). The matrix enclosing the specimen differs from that seen in other Lealt Shale Formation pterosaurs including the *Dearc* holotype (NMS G.2021.6), with less pyritic growth, less shelly material and poorer cementation. The preservation style is also different, with NMS G.2023.1.1 exhibiting a greater degree of disarticulation and flattening.

*Locality and preparation.* The fossil was found in the Lonfean Member of the Lealt Shale Formation (Bathonian, Middle Jurassic) at the headland of Rubha nam Brathairean (Brothers’ Point) (Fig. 1) on the Trotternish peninsula, Isle of Skye, Scotland [NG 52454 62032]. The fossil was discovered, collected and prepared (in the University of Edinburgh Deep Time prep lab) by TJC.

### Description

The bones were partially prepared from the limestone block but have been kept *in situ* rather than being completely removed (Fig. 2a–c). The long bones are fractured with obscured articulation facets but retain much of the original dimensions. The caudal elements, however, are crushed and therefore laterally expanded.

### Caudal vertebrae

The preserved caudal section collectively measures 100 mm in length (Fig. 2a–c), with at least two distinguishable vertebrae. Although they are crushed, the vertebrae appear relatively robust and large. The anterior-most caudal is 25 mm long, with a width measuring 4 mm across the centrum and 5 mm at its slightly flared ends. The bone is crushed and slightly deformed, which might inflate its dimensions. The ratio of width/length is 6.3, which in some non-pterodactyloid pterosaurs (e.g. *Campylognathoides liasicus*, SMNS 50735; *Darwinopterus modularis*, ZMNH M8782 and (Wellnhofer 1975) Nr. 68 *Rhamphorhynchus muensteri*) indicates a position in the anterior mid-section of the tail, and probably does not represent the longest element. One has to bear in mind, however, that the deformation of these features prevents measurements from being definitive. The caudal vertebrae are flanked by strut-like filiform processes similar in thickness (0.5 mm), with the longest uninterrupted segment being 30 mm long. All lie parallel to the vertebrae with occasional thicker (1.2 mm) elements possibly belonging to zygapophyses.

### Tibiotarsus

The identification of this bone as a tibiotarsus is based on its morphological features, along with circumstantial evidence of its proximity to the metatarsal and caudal vertebral elements. The shaft is long and straight, and does not undulate in thickness throughout its length, but expands only at the distal apex, at the region with condyles. This is characteristic of pterosaur tibiotarsus bones (Galton 1980; Baird and Galton 1981). Moreover, this shape is unlike what would be expected in other pterosaur long bones such as femora (Wellnhofer 1975; Padian 2008) (Fig. 2a–c), which tend to possess sigmoidal or concave diaphyseal curvature. Femora also generally become wider distally, with the

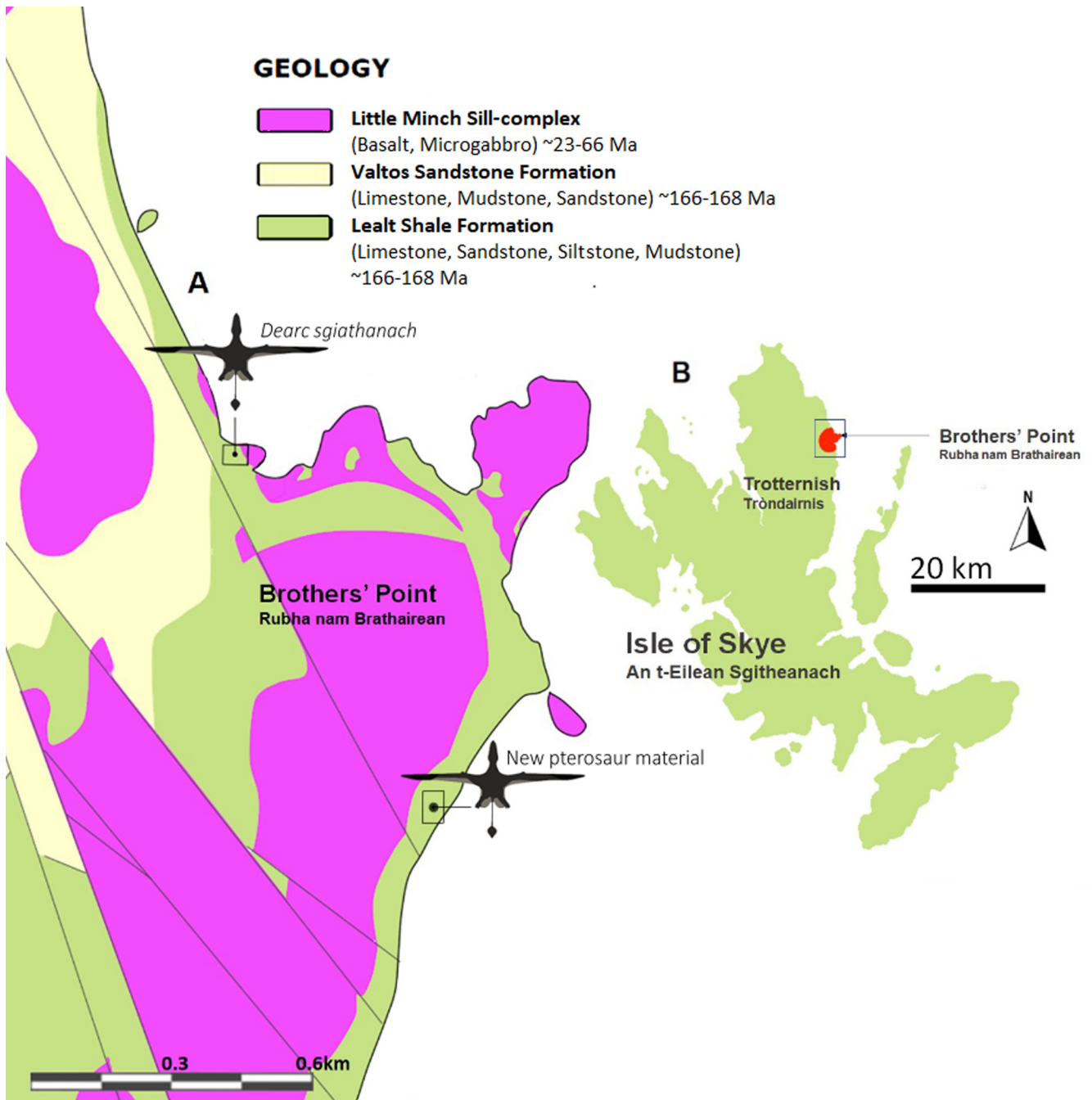


**Fig. 1.** Location of pterosaur remains on the Brothers' Point headland. (a) Geological map of the headland with locations of pterosaur remains. Scale bar: 0.6 km. (b) Location of the headland in relation to entirety of Isle of Skye. Scale bar: 20 km.

diaphysis body widening to reach the apex width of the condyles; this is the case from early diverging pterosaurs such as *Raeticodactylus* (BNM 14524) (Stecher 2008) as well as derived dsungaripterids (such as DFMMh/FV 500) (Fastnacht 2005). Other straight long bones include wing phalanges, which tend to be oval in cross-section and have simple, flat articular apices. Ulna and radius also are sizeable, straight-shafted appendicular bones; these too can show modulations in diaphysis, have an oval cross-section elongate along a single long axis and lack bicondylar structure, with an accentuated trochanter and olecranon, which are invisible in this specimen. A bicondylar distal end is also found in metacarpals, albeit this feature tends to be short and wide in long-tailed Jurassic pterosaurs, with usually a medial sulcus creating a broad U-shaped cross-

section. The condyles are also enlarged with flat lateral surfaces, not visible in our specimen.

The assumed element of the right distal tibiotarsus retains a sizeable portion of the diaphysis and distal condyles and misses the proximal articulation region. The bi-condylar apex makes us speculate the elements possibly belong to the distal part of the tibia, albeit its poor preservation warrants caution in this identification.

The preserved segment of the tibiotarsus (Fig. 2a–c) is 82.8 mm long; of this, 65 mm is present as bone, with the remaining part of the diaphysis proximally persisting as an impression in the slab (17.8 mm). The element is nearly circular (5.3 mm by 4.8 mm) at the anterior medial cross-section where it is broken proximally. The bone is 5.3 mm thick at the medial section of the diaphysis, expanding from

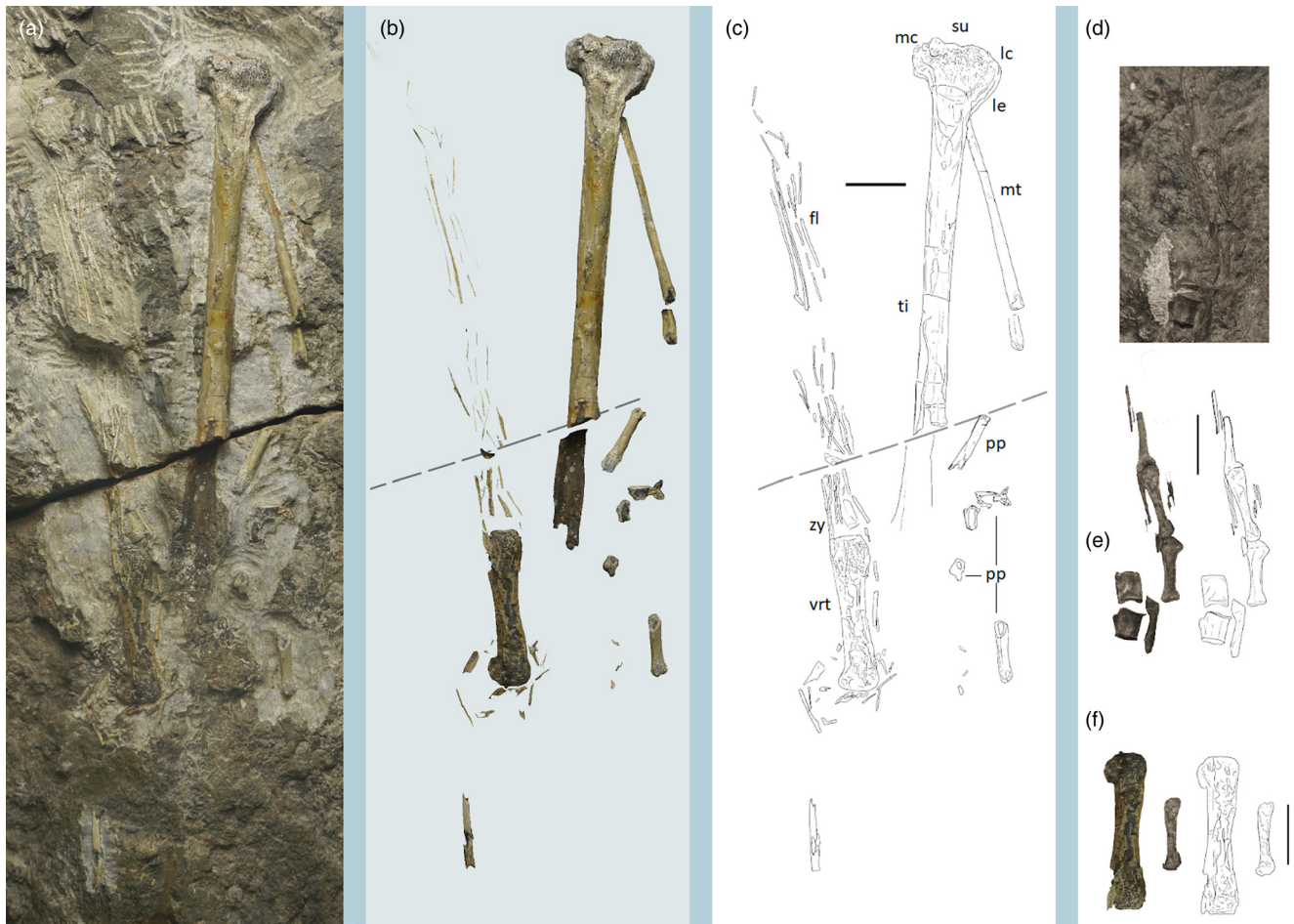


**Fig. 2.** (a) Photograph of the NMS G.2023.1.1 slab; (b) bone separated digitally from the matrix; (c) annotated line drawing; (d) photograph of anterior caudal of NMS G.2021.6 (*Dearc*); (e) digitally separated and annotated line drawing of the caudal segments of NMS G.2021.6 (*Dearc*); (f) size comparison, photograph and line drawing, left NMS G.2023.1.1 and right NMS G.2021.6 (*Dearc*). fl, filiform; lc, lateral condyle; le, lateral epicondyle (?); mc, medial condyle; mt, metatarsal; pp, pedal phalanges; su, sulcus; ti, tibia; vrt, caudal vertebrae; zy, zygapophyses. Scale bar: 10 mm.

7.3 to 15.3 mm at its distal end, of which 4.3 mm belongs to the lateral condyle and 6.9 mm to the medial (fibrotarsal) condyle. The bone walls of the diaphysis in cross-section are 1.2 mm thick (out of a 5.3 mm total diameter at the point of the fracture), giving an *R/t* (outer radius to bone wall thickness, from [Fastnacht 2005](#)) ratio of 2.2. This is typical for non-pterodactyloid bone walls ([Fastnacht 2005](#)), similar to the condition observed in *Dearc* (1.9–2.5).

The two distal condyles are separated by a very shallow U-shaped sulcus. The identifications of medial and lateral condyles are uncertain given the crushing and doubt regarding preservation orientation. The putative medial condyle has an elevated rugosity on its surface, although this might be due to taphonomic damage. The supposed medial condyle protrudes from the diaphysis medially at a right angle; the lateral condyle deflects from the long axis of the diaphysis at a 150° slope. There is a protrusion close to the lateral condyle, which is either a taphonomic artefact or a genuine lateral epicondyle, which would reach the calcaneum part of the fused tibiotarsus; it has two spatula-shaped bulbous ends and a total thickness of 2.3 mm. The tibiotarsus in later growth stages ossifies the calcaneum and astragalus to form a unified distal condyle (as in [Andres et al. 2010](#)) ([Fig. 3a](#)). The calcaneum and astragalus on NMS G.2023.1.1 appear fully ossified, indicating that this individual was unlikely to be a juvenile. There is a texture change close to

where condyles and diaphysis meet, with the condyles having a mottled texture differing from the smooth diaphysis. In the distal profile view, the assumed medial condyle is bigger than the lateral condyle; the assumed lateral condyle is flat, whereas the medial condyle appears bulbous and tall. A shallow groove on the diaphysis surface posterior to the condyles probably acted as an attachment for the *ligamentum obliquum*. The depression under the medial condyle and distally expanded diaphyseal sides possibly hosted the *musculus extensor digitorum longus* ([Padian 1983](#)), which aided flexing of the pedal digits. This is all largely assumed, as even the orientation of the bone element is questioned owing to its fragmentary and poor preservation.

### *Metatarsal and digits*

A single metatarsal and select pedal phalange elements are present and positioned proximal to the tibiotarsus ([Fig. 2a–c](#)). The incomplete metatarsal has a total preserved length of 42.4 mm; the proximal articular end is concealed by the tibia and the distal end is fractured. The metatarsal has no visible articulation facet and has a uniform thickness of 2.6 mm. The bone walls are thick (1 mm), with a small pinhole for the medullary cavity. The non-pterodactyloid pterosaur pedal phalangeal formula is 2-3-4-5-2 ([Witton 2013](#)). Given there are three to four partial, short, phalange-like elements distal

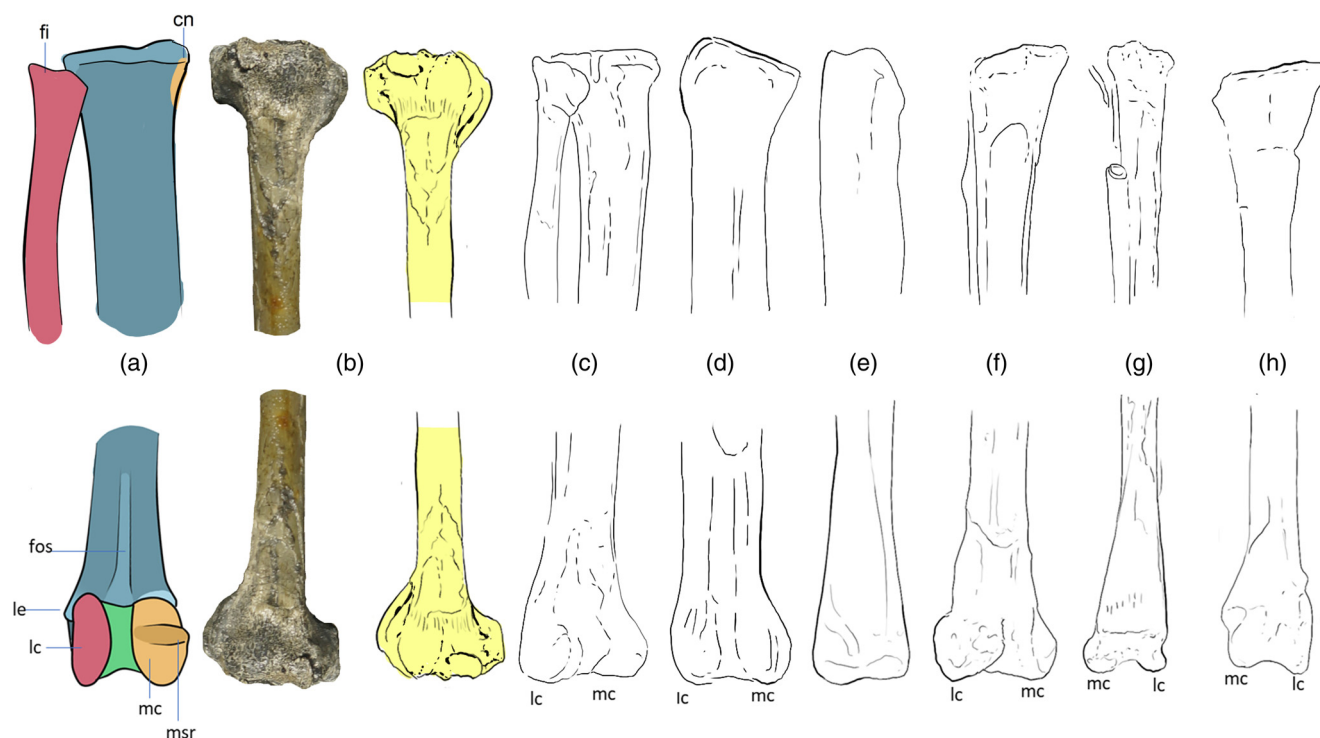


**Fig. 3.** Proximal (top) and distal (bottom) ends of tibiotarsi in anterior view. (a) Model colour-coded proximal (top) and distal (bottom) tibiotarsi after *D. macronyx*; (b) NMS G.2023.1.1 photograph and interpretative illustration of long bone termination with darker outline showcasing areas of taphonomic flaking; (c) NHMUK PV OR 43051, *Dimorphodon*; (d) left (proximal), right (distal) NHMUK PV OR 41212, *Dimorphodon*; (e) MOZ -PV -094, pterodactyloid; (f) NHMUK PV OR 42737, unidentified; (g) NHMUK PV R 2786 *Rhamphorhynchus*; (h) NHMUK PV R 9191 *Dsungaripterus* sp. cn, cnemial crest; fi, fibula; fos, diaphysis bearing fossa; lc, lateral condyle; le, lateral extremity; mc, medial condyle; msr, medial condyle rugosity. Not to scale.

to the metatarsal, the bones may represent those of digit 3 or 4. The disarticulated, medially eroded metapodial phalangeal elements measure 11.4, 10.7 and 10.4 mm respectively. These are tubular and no thicker than 2.4 mm.

### Comparative assessment

#### *Comparisons of new material with known Jurassic pterosaur caudal vertebrae*

Caudal vertebrae vary considerably in pterosaurs. In non-pterodactyloid pterosaurs, the caudal series is elongate and usually supported by stiffening processes (although not seen in every genus; Hone *et al.* 2012), whereas pterodactyloids tend to have a reduced tail (Lü and Hone 2012). Basal Triassic pterosaurs such as *Eudimorphodon* or *Austriadactylus* have considerably more robust caudal bones than more derived non-pterodactyloids (Dalla Vecchia *et al.* 2002; Dalla Vecchia 2013). For example, SMNS 56342, *Austriadactylus cristatus* holotype, notably lacks the stiffening ‘bony sheath’, having reduced zygapophyses and hemal arches. The individual caudal vertebrae are elongate and thick, with the longest mid-section (ninth) caudal being 28 mm long and 4.2 mm thick, comparable with the thickness of tibia (4.4 mm), in an animal of estimated wingspan no larger than 1.2 m. In size and dimension, SMNS 56342 is most comparable with, if not bigger than, NMS G.2023.1.1, albeit the bony sheath in the Scottish specimen is dissimilar to the morphotype of the Triassic pterosaur, with filiform composed of numerous elongate, thin chevrons. The caudal bones were reduced in size and increased in number in Jurassic pterosaurs, even sizeable non-pterodactyloid pterosaurs, such as

*Rhamphorhynchus muensteri* (NHMUK PV OR 37002), with thin and slender caudals (0.5 mm by 14 mm at the caudal mid-section), where the surrounding filiform is thicker than the tail bone itself, which differs from the condition in NMS G.2023.1.1. In the new material, the filiform is longer than the length of the caudal bone, but considerably thinner.

The non-pterodactyloid caudal elements become somewhat conservative in the Jurassic. Exceptions include anurognathids and select species, such as the juvenile holotype *Bellubrunnus rothgaengeri* (Hone *et al.* 2012; Lü and Hone 2012), with caudals being reduced and squat, with relatively flat margins of the centrum, and reduced chevrons (three times caudal centra) with short pre- and postzygapophyses.

Elongate and rod-like extensions of the zygapophyses and chevrons, supported tails are also characteristic to Wukongopterids, such as *Kunpengopterus sinensis* (IVPP V 23674), with the maximum length reached at the sixth caudal, with length of 12.6 mm (Cheng *et al.* 2017) and 1.3 mm width, being 23% of tibia length. The thickness of the caudal is comparable with that of preserved tibia (1.7 mm), similar to our specimen. However, in *Jianchangopterus zhaoianus* (YHK-0931) (Lü and Bo 2011), a juvenile wukongopterid, the caudals are considerably thinner than the tibiotarsus, pointing at ontogenetic variability of this feature, rendering it undiagnostic. The supporting filiforms in sampled wukongopterids are comparable in thickness with the body of the caudal bone, dissimilar to NMS G.2023.1.1. With limited described material and no sizeable wukongopterids, it is hard to confirm if our pterosaur falls within this clade.

The elongate, rectangular filiform-supported caudal series of NMS G.2023.1.1 warrants a non-pterodactyloid

identification, but it differs markedly from similar-sized pterosaurs from Solnhofen, with morphology akin to the basal Triassic pterosaurs, with markedly different stiffening processes, preventing narrowing down the assessment to known taxa.

### Comparisons of new material with known Jurassic pterosaur tibiotarsi

Given the amount of three-dimensionally preserved sizeable Jurassic pterosaur tibias is sparse, we decided to compare the novel Scottish specimen with the limited analogous material in the literature. Not many comparative studies have focused on Jurassic pterosaur tibiotarsi, except those by Galton (1980) and Padian (1983), who both noted similarities between the distal tibiotarsus of pterosaurs and those of birds. Galton (1980) wrote about the attachment area for a transverse ligament, lateral and medial ligamentous prominences, and a pulley-like anteroposterior sulcus in Kimmeridgian–Tithonian material from the Tendaguru Formation in Tanzania, stored in London. Galton (1980) considered the African pterosaur material to be closely related to Chinese *Dsungaripterus weii*. The condyles from Tendaguru pterosaurs (identified as *Dsungaripterus* sp.) (Fig. 3h) do not protrude laterally and have a shallower separating sulcus. NHMUK PV R 9191 (Galton 1980) (Fig. 3h), like NMS G.2023.1.1, exhibits a protrusion stemming from the lateral condyle, in distal view. However, our NMS G.2023.1.1 appears much flatter in the distal cross-section view than the bones featured in the assessment by Galton (1980). The tibiotarsi (featured in Galton's (1980) paper) are long (105 mm total for FML 3869 (*Puntanipterus*

*globus*) to 126 mm in HMN Nr.1 (*Dsungaripterus* sp.)) but markedly different from those of NMS G.2023.1.1. This variation is indicative of distal condyles having discernible features and condyle shapes corresponding to differences in function, which are outside the scope of this paper. It also indicates that NMS G.2023.1.1 differs from derived Tendaguru species and pterodactyloids, despite having similar dimensions. Another tibiotarsus comparable in size (214 mm long) with NMS G.2023.1.1 is an isolated specimen, MOZ-PV-094 (Codorniu and Garrido 2013) (Fig. 3e) from Argentina. The bone is preserved in anterior view and is associated with proximal tarsals and a fused fibula. The bone is sizeable and expanded anteriorly owing to periosteal calcification covering a bone fracture. The bone has an oval, albeit crushed, cross-section, different from the Tendaguru specimens. Unlike NMS G.2023.1.1 the condylar ends are considerably less flared, but like NMS G.2023.1.1 the sulcus remains shallow.

The Lower Jurassic *Dimorphodon macronyx* is known from numerous tibiotarsal elements, well preserved in distal and anterior views (e.g. NHMUK PV OR 43051 and NHMUK PV OR 41212) (Sangster 2021) (Fig. 3c and d). NHMUK PV OR 43051 has an interosseous gap (a furrow left by the fusion of the fibula to the tibia diaphysis) terminating at the lateral edge of the distal trochlea, similar to NMS G.2023.1.1. NHMUK PV OR 43051 (Fig. 3c) has an oval depression for foot tendons, and a shallow trochlear groove, probably occupied by the *m. gastrocnemius*, possibly visible in the Scottish specimen. In NHMUK 43051 (Fig. 3c) the lateral condyle curves, accommodating the passage of tendons to the foot. The lateral condyle is narrow relative to the medial condyle, and protrudes anteriorly prominently,

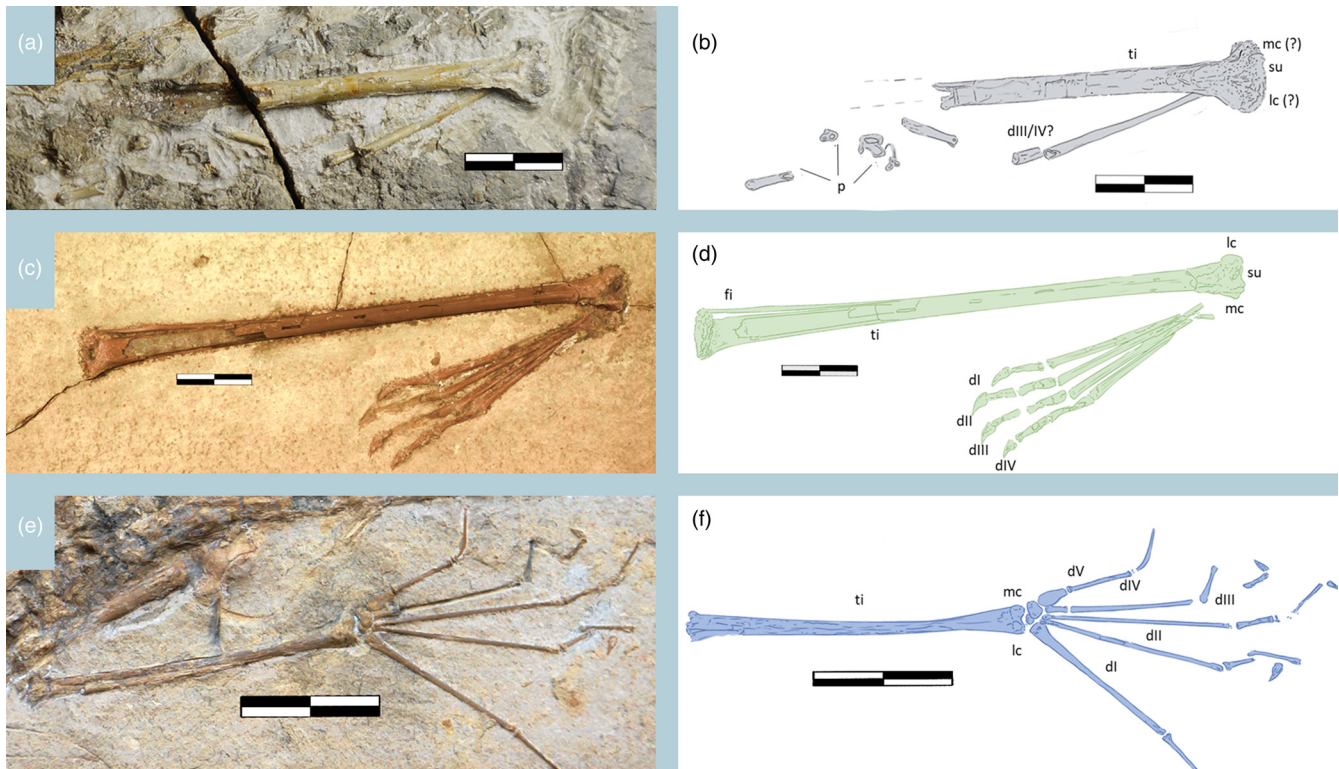


**Fig. 4.** Comparison of select tibiotarsal and pedal elements; (a, c, e) photographs; (b, d, f) annotated line drawings; (a, b) NMS G.2023.1.1, the new Scottish material; (c, d) unassigned NHMUK PV OR 42737; (e, f) *Rhamphorhynchus*, NHMUK PV R 2786. Scale bar: 20 mm. d#, digit; fi, fibula; lc, lateral condyle; mc, medial condyle; p, pedal phalanges; su, sulcus; ti, tibia.

similar to the condition in NMS G.2023.1.1. The medial condyle retains an elevated striation used for digit extension. Another Toarcian pterosaur, *Campylognathoides zitteli* (holotype, SMNS 9787) (Padian 2008), has a slope from diaphysis to the medial condyle as in NMS G.2023.1.1, but does not have the same degree of distal expansion.

The Late Jurassic Solnhofen Plattenkalk deposits have produced numerous articulated, fully preserved pterosaur skeletons, although many of these are small, immature individuals with distal ends of the tibiotarsi either unossified or replaced by mass calcium (Bennett 1996). Some specimens retain characteristic features, such as an isolated pes (NHMUK PV OR 42737) (Fig. 3f), warranting a comparison with our material (Fig. 4). The tibia associated with this pes is 143 mm long and expands proximally, being 50 mm wide at the distal diaphysis (Fig. 4c and d). The size of elements is large for a Solnhofen pterosaur. Like NMS G.2023.1.1, anterior to condyles it bears a furrow, but it then shows a transition to a ridge distally, differing from the new Skye specimen. The clade assignment of NHMUK PV OR 42737 has shifted with time, from *Pterodactylus* to *R. muensteri* (Steel 2012) (NHM data portal: NHMUK: ecatalogue: 483084). As in NMS G.2023.1.1, the tibiotarsus is preserved and is long and straight. The condyles are not as laterally expanded as in NMS G.2023.1.1 but retain a shallow sulcus.

Two tibiotarsi are also present in the well-preserved small *Rhamphorhynchus* individual, NHMUK PV R 2786 (Fig. 3g and Fig. 4e, f). Unlike other small pterosaurs of this genus, the distal end is fully ossified and not replaced with calcite crystal growth. The medial condyle of the right tibiotarsus is enlarged, relative to the lateral, but both are small, featureless and undeveloped. Thus, immaturity is visible, even when the element ossifies to the diaphysis. This suggests that NMS G.2023.1.1 was in a later growth stage compared with NHMUK PV R 2786 (Fig. 4).

Summarizing, there is no clearly analogous tibiotarsus to NMS G.2023.1.1. It differs strikingly from material of larger early pterodactyloids and shows some similarities to the Early Jurassic non-pterodactyloid forms, but otherwise, with flared asymmetrical distal condyles, it cannot be unambiguously compared with elements currently present in the literature.

#### **Comparisons of new material with known Jurassic pterosaur metatarsals**

The metatarsal of NMS G.2023.1.1 has a thickness of 2.6 mm. The 2 mm thickness is not exceeded in other known pterosaurs, seen in the large Jurassic hindlimb NHMUK PV OR 42737 (*Dimorphodon macronyx*), the largest preserved Solnhofen specimen of *Rhamphorhynchus* (NHMUK PV OR37002) and the holotype of *Dearc* (NMS G.2021) (expanded on in the subsection below). This suggests that NMS G.2023.1.1 belongs to either a considerably larger individual compared with the largest known non-pterodactyloid pterosaurs (including Wukongopterids) or a new species with a robust morphology.

#### **Comparing the new material with other Scottish pterosaur remains**

The first formally described pterosaur fossil from Scotland, a single undiagnostic wing phalanx (WP2 or WP3), originates

from Late Jurassic (Kimmeridgian) deposits of Eathie (Ross and Cromarty, north of Inverness) (NHMUK PV R1362) (Steel and O'Sullivan 2015). The bone is 125 mm long, although the impression of the missing articular ends renders its total length 160 mm, giving an estimated wingspan between 1.6 and 1.8 m (Steel and O'Sullivan 2015). The phalanx has a shallow groove on the caudal surface of the shaft, indicative of an affinity to a *Rhamphorhynchus* (Steel and O'Sullivan 2015). This specimen comes from Late Jurassic deposits, younger than the Middle Jurassic fossil we are describing here, but showcases that we already knew that Scottish seaways were once inhabited by non-pterodactyloid grade pterosaurs with sizeable wingspans.

*Dearc sgiathanach* is the only other pterosaur from the Lealt Shale Formation yet described. However, despite the overall excellent preservation of the holotype skeleton, its tibiotarsi were lost to tidal erosion (Jagielska *et al.* 2022), and thus we cannot make direct comparisons with NMS G.2023.1.1. The metatarsal in NMS G.2023.1.1, however, is thicker than the ones described in *Dearc* (NMS G.2021.6), and seemingly does not exhibit the autapomorphic condition of the fourth metatarsal of *Dearc* (*a tabular morphology, which makes it considerably thicker than metatarsals 1–3*) (Jagielska *et al.* 2022). The medial thicknesses of metatarsals 1–3 in *Dearc* vary from 1.65 to 1.2 mm, which is half the corresponding measurement in the new Skye specimen. This suggests that NMS G.2023.1.1 belongs to an individual with a larger, more robust pes than the holotype individual of *Dearc*.

The size discrepancy between NMS G.2023.1.1 and the *Dearc* holotype is also apparent in the caudal elements (Fig. 2d–f). In *Dearc*, the anterior-most ‘rudder’ caudals measure 6.6 by 5.1 mm (ratio of length to width is 1.29) and 10 by 3.3 mm (ratio of length to width is 3), whereas the only complete caudal from the elongated tail section has a ratio of 4.62, based on dimensions of 15.7 and 3.4 mm of the small bone. The bone preserved in NMS G.2023.1.1, despite being crushed, is considerably larger than the one in *Dearc*. The element is also visually different, as it is more oblate than the rectangular bone in *D. sgiathanach*. In interpreting these differences, one has to consider that the two caudal vertebrae are poorly preserved and of unknown definitive location within the caudal section. No detailed comparative studies on caudal bones in non-pterodactyloid pterosaurs have been conducted thus far. This might be due to the caudal section usually being hard to compare, given the filiform projections covering individual bones and disarticulation that prevents easy assignment to a particular segment of the tail. The segment in NMS G.2023.1.1 is too short and poorly preserved to allow for a more detailed assessment. Therefore, in overall appearance, it adds to evidence from the metatarsal that NMS G.2023.1.1 is probably from a larger individual than the *Dearc* holotype.

We can compare NMS G.2023.1.1 with one final specimen from the Isle of Skye, a tibiotarsus from a non-pterodactyloid collected from the Kilmaluag Formation and briefly mentioned and illustrated by Panciroli *et al.* (2020, fig. 8d) in their review of the Kilmaluag Formation. The two bones are similar in overall appearance, with similar dimensions of the medial diaphysis with a width of 6.7 mm, changing to 15 mm at the condyle. As in NMS G.2023.1.1, the Kilmaluag specimen has a leading edge

leading to the formation of a condyle. Although it is not fully prepared and described to allow full comparison, it might represent a similar species.

In summary, although the new Lealt Shale Formation specimen NMS G.2023.1.1 is highly incomplete, we can make several solid inferences about its affinities. It is clearly a non-pterodactyloid, because of its elongated tail with stiffening processes. It has an unusual distal condyle of the tibiotarsus, with both condyles notably protruding from the diaphysis, and a poorly defined shallow sulcus separating asymmetrical condyles, which is unknown in any other Jurassic pterosaurs to our knowledge, but which may be similar to the condition in a still-undescribed Skye specimen illustrated by [Pancioli \*et al.\* \(2020, fig. 8d\)](#). The preserved elements of NMS G.2023.1.1, particularly the metatarsal but possibly also the caudal vertebrae, are suggestive of an individual larger than the holotype skeleton of *D. sgiathanach* (NMS G.2021.6), an immature individual whose wingspan was estimated at greater than 2.5 m ([Jagielska \*et al.\* 2022](#)), making it the largest known Jurassic pterosaur with a reasonably confident wingspan estimate. It may be that NMS G.2023.1.1 is an older and larger individual of *Dearc*, or a new genus and/or species. The unusual tibiotarsal condyle feature mentioned could potentially be a diagnostic feature of a new genus and/or species, or an unrecognized autapomorphy of *Dearc* that has not yet been noticed because of the lack of tibiotarsi in the holotype. Because of the difficulty in distinguishing these two possibilities, we have decided not to give the new specimen a genus or species name.

## Discussion

Sampling biases alter the way we perceive tetrapod diversity and distribution over time ([Benson and Butler 2011](#)), and this is especially true of pterosaurs, whose fragile bones and lightweight skeletons were difficult to preserve as fossils ([Butler \*et al.\* 2012, 2013](#); [Benson \*et al.\* 2014](#); [Dean \*et al.\* 2016](#)). Our understanding of pterosaur evolution is plagued by the ‘Lagerstätten effect’, as so much of our knowledge comes from fossils preserved in exceptional settings with exquisite preservation ([Butler \*et al.\* 2013](#); [Dean \*et al.\* 2016](#)). These lagerstätten, therefore, may be a false representation of diversity or speciation and provide no convincing statistical support for biogeographical patterns in species dispersal or endemism ([Upchurch \*et al.\* 2015](#)). Preservation biases will favour the preservation of certain skeletal elements over others. Simply put, all pterosaurs bore full skeletons in life, but fossils often show a strong preference for the preservation of select elements, such as forelimbs (as seen in the Great Oolite Group, England) ([O’Sullivan and Martill 2018](#)) or rostra (as seen in the Kem Kem Group, Morocco) ([Smith \*et al.\* 2022](#)), with geographical biases ([Barrett \*et al.\* 2008](#); [Upchurch \*et al.\* 2015](#)) favouring Laurasian pterosaurs, although that is changing with increasing discoveries coming from the southern continents ([Alarcón-Muñoz \*et al.\* 2020](#)).

Pterosaur-bearing lagerstätten are not perfect snapshots of individual pterosaur faunas, much less accurate records of pterosaur evolution and diversity over time. These exceptionally preserved sites often show a preference for pterosaurs of certain sizes, habitats and clades. For

example, Cretaceous sites exhibit a preference for the preservation of sizeable and osteologically mature taxa ([Smith \*et al.\* 2022](#)), in contrast to those of the Jurassic and Triassic, which are dominated by small (less than 2 m wingspan), usually juvenile pterosaurs found in marine and lagoonal deposits ([Bennett 1996](#); [Smith \*et al.\* 2022](#)). This, in part, has led to the argument that pterosaurs substantially increased in size and terrestrial affinity with the diversification of the pterodactyloid clade since the Late Jurassic ([Witton 2015](#)). Preservation biases also painted a picture of a long-term diminishing of pterosaur diversity and distribution before the end-Cretaceous extinction ([Longrich \*et al.\* 2018](#); [Yu \*et al.\* 2023](#)).

New work, especially detailed study of individual pterosaur-bearing fossil sites, is helping to understand these sampling biases and is leading to a more accurate understanding of major trends in pterosaur evolution. The recent review of numerous fragmentary elements from the Mid-Cretaceous Kem Kem Group points to unseen taxonomic and size diversity ([Smith \*et al.\* 2022](#)), in a period previously thought to be dominated by pterosaurs of limited size range and taxonomic affinity. This has been achieved via improvements in determining maturity and the ability to assign a genus even to partial material ([Smith \*et al.\* 2022](#)). Substantial fragmentary material from the Jurassic has been reassessed in recent decades ([Kellner \*et al.\* 2007](#); [O’Sullivan and Martill 2018](#); [Alarcón-Muñoz \*et al.\* 2020](#)), and assigned grade, genus or species identifications, especially from locations and environments outside the exceptional lagerstätten. The study of partial material from Britain ([O’Sullivan and Martill 2017, 2018](#)), Tendaguru ([Costa and Kellner 2009](#)) and South America ([Rauhut and López-Arbarello 2008](#)) illuminates a higher diversity of pterosaurs during the Jurassic than previously thought, including the unexpected appearances of derived clades, such as a supposed early azhdarchid ([Kellner \*et al.\* 2007](#)), and a much wider size range than previously recognized ([Jagielska \*et al.\* 2022](#)). This exemplifies the importance of describing fragmentary specimens from outside lagerstätten and including partial material in wider macroevolutionary studies.

The new specimen described here, NMS G.2023.1.1, demonstrates that *Dearc* ([Jagielska \*et al.\* 2022](#)) was not anomalous. In other words, it corroborates the hypothesis that numerous morphologically robust and sizeable pterosaurs were commonplace in the Middle Jurassic of Britain. Along with the Great Oolite collections from England, the new discoveries from Skye reveal that the European Middle Jurassic fossilized pterosaur assemblages differ in size, from individual specimens with wingspans below 1 m to above 3 m ([Jagielska \*et al.\* 2022](#)), and in clades represented ([O’Sullivan and Martill 2018](#)). Bathonian Great Oolite material includes elements with clade-diagnostic features, indicating taxa such as potential scaphognathins (flared, stout mandibular symphysis GSM 113723, bearing a resemblance to PMOL-AP00028 *Jianchangnathus robustus* ([Bennett 2014](#); [Zhou 2014](#))), rhamphorhynchids (based on a pair of large, slender mandibles (NHMUK PV R 1824) and furrowed phalanges), early monofenestratans (based on cranial material (NHMUK PV R 464), similar to *Cuspicephalus scarfi* ([Martill and Etches 2012](#))) and potentially even pterodactyloids. The European Middle Jurassic deposits are now characterized by



clades similar to other known diverse assemblages that boast much more complete and well-preserved material, such as the Late Jurassic Tiaojishan or Solnhofen Formation (Bennett 1996; Lü *et al.* 2010; Sullivan *et al.* 2014; Zhou 2014; Zhou *et al.* 2021). Some of the only remaining differences are that anurognathids and a high diversity of ctenochasmatids and other pterodactyloids are not (yet) seen in the Middle Jurassic of Europe (Bennett 1996; Zhou *et al.* 2017; O’Sullivan and Martill 2018).

## Conclusion

NMS G.2023.1.1 provides further evidence that sizeable non-pterodactyloid pterosaurs inhabited the marginal-marine deposits of the Tethyan–Boreal seaway in the Middle Jurassic. The new fossil belongs to a larger, more robust specimen than the holotype of *Dearc sgiathanach*, a pterosaur recently described from the same rock unit (Lealt Shale Formation) and identified as having the largest wingspan (>2.5 m) of any well-known Jurassic pterosaur (Jagielska *et al.* 2022). The new Lealt Shale Formation pterosaur, although highly fragmentary, shows that the discovery of *Dearc* was not anomalous. There were large pterosaurs that flew over the heads of dinosaurs during the Middle Jurassic, and the Bathonian seaway stretching from contemporary England to the Hebrides was populated by a diversity of species, of varying sizes and taxonomic affinities. As the Lealt Shale Formation has only recently begun to yield pterosaur fossils, more specimens probably remain to be found.

## Institutional abbreviations

BNM, Bündner Naturmuseum, Chur, Switzerland; DFMMh, DinoPark Münchenhagen, Germany; FML, Fundación Miguel Lillo, Tucuman, Argentina; GSM, British Geological Survey, Keyworth, UK; HMN, Humboldt Museum für Naturkunde, Berlin, Germany; IVPP, Institute of Vertebrate Paleontology and Paleoanthropology, Beijing, China; MOZ-PV, Museo Provincial de Ciencias Naturales, Neuquén, Argentina; NHMUK, Natural History Museum London, UK; NMS, National Museums Scotland, Edinburgh, UK; SMNS, Staatliches Museum für Naturkunde, Stuttgart, Germany; ZMNH, Zhejiang Museum of Natural History; YHK, Yizhou Museum, China; PMOL, Paleontological Museum of Liaoning, Shenyang Normal University, Shenyang, China.

## Scientific editing by Yves Candela

**Acknowledgements** We thank W. Juszcak for help during photography, S. Walsh for curation support at National Museums Scotland, E. Martin-Silverstone for discussion and our 2017 field crew (P. dePolo, D. Foffa, D. Goldberg, J. Hoard, M. Johnson, S. Marrero, A. McGowan, M. Ogunkanmi, E. Panciroli, P. Pereira, A. Ross, S. Walsh, and Wheelbarrow Steve). We thank our peer reviewers for invaluable feedback, Drs Dave Hone and Jordan Bestwick.

**Author contributions** NJ: formal analysis (lead), investigation (lead), methodology (lead), visualization (lead), writing – original draft (lead), writing – review & editing (supporting); TJC: conceptualization (supporting), data curation (supporting), resources (equal), writing – review & editing (supporting); MO: formal analysis (supporting), methodology (supporting), supervision (supporting), writing – review & editing (supporting); DAR: data curation (supporting), resources (supporting); NCF: data curation (supporting), writing –

review & editing (supporting); MW: writing – review & editing (supporting); SLB: funding acquisition (supporting), supervision (lead), writing – review & editing (supporting)

**Funding** We acknowledge funding from the Natural Environment Research Council E4DTP studentship (NE/S007407/1) to NJ, the National Geographic Society (GEFNE185-16 to PI SLB) which funded fossil excavations on Skye, and a Philip Leverhulme Prize to SLB, which funded Edinburgh’s palaeontological laboratory.

**Competing interests** The authors declare that they have no known competing financial interests or personal relationships that could have appeared to influence the work reported in this paper.

**Data availability** The analysed material in the current study is available in the National Museums Scotland collections. All data generated or analysed during this study are included in this published article.

## References

- Alarcón-Muñoz, J., Otero, R.A., Rojas, O. and Rojas, J. 2020. Los pterosaurios de Chile: Su descubrimiento y estado actual del conocimiento. *Museo de Historia Natural y Cultural del Desierto de Atacama, Publicación Ocasional*, **3**.
- Alarcón-Muñoz, J., Otero, R.A., Soto-Acuña, S., Vargas, A.O., Rojas, J. and Rojas, O. 2021. First record of a Late Jurassic rhamphorhynchine pterosaur from Gondwana. *Acta Palaeontologica Polonica*, **66**, 571–583, <https://doi.org/10.4202/app.00805.2020>
- Andres, B., Clark, J.M. and Xing, X. 2010. A new rhamphorhynchid pterosaur from the Upper Jurassic of Xinjiang, China, and the phylogenetic relationships of basal pterosaurs. *Journal of Vertebrate Paleontology*, **30**, 163–187, <https://doi.org/10.1080/02724630903409220>
- Baird, D. and Galton, P.M. 1981. Pterosaur bones from the Upper Cretaceous of Delaware. *Journal of Vertebrate Paleontology*, **1**, 67–71, <https://doi.org/10.1080/02724634.1981.10011880>
- Barrett, P.M., Butler, R.J., Edwards, N.P. and Milner, A.R. 2008. Pterosaur distribution in time and space: an atlas. *Zitteliana*, 61–107.
- Barron, A.J.M., Lott, G.K. and Riding, J.B. 2012. *Stratigraphical Framework for the Middle Jurassic Strata of Great Britain and the Adjoining Continental Shelf*. British Geological Survey.
- Beardmore, S.R., Lawlor, E. and Hone, D.W.E. 2017. Using taphonomy to infer differences in soft tissues between taxa: an example using basal and derived forms of Solnhofen pterosaurs. *Science of Nature*, **104**, 1–11, <https://doi.org/10.1007/s00114-017-1486-0>
- Bennett, S.C. 1995. A statistical study of *Rhamphorhynchus* from the Solnhofen Limestone of Germany: year-classes of a single large species. *Journal of Paleontology*, **69**, 569–580, <https://doi.org/10.1017/S0022336000034946>
- Bennett, S.C. 1996. Year-classes of pterosaurs from the Solnhofen Limestone of Germany: taxonomic and systematic implications. *Journal of Vertebrate Paleontology*, **16**, 432–444, <https://doi.org/10.1080/02724634.1996.10011332>
- Bennett, S.C. 2014. A new specimen of the pterosaur *Scaphognathus crassirostris*, with comments on constraint of cervical vertebrae number in pterosaurs. *Neues Jahrbuch für Geologie und Paläontologie, Abhandlungen*, **271**, 327–348, <https://doi.org/10.1127/0077-7749/2014/0392>
- Benson, R.B. 2018. Dinosaur macroevolution and macroecology. *Annual Review of Ecology, Evolution, and Systematics*, **49**, 379–408, <https://doi.org/10.1146/annurev-ecolsys-110617-062231>
- Benson, R.B. and Butler, R.J. 2011. Uncovering the diversification history of marine tetrapods: ecology influences the effect of geological sampling biases. *Geological Society, London, Special Publications*, **358**, 191–208, <https://doi.org/10.1144/SP358.13>
- Benson, R.B., Frigot, R.A., Goswami, A., Andres, B. and Butler, R.J. 2014. Competition and constraint drove Cope’s rule in the evolution of giant flying reptiles. *Nature Communications*, **5**, 1–8, <https://doi.org/10.1038/ncomms4567>
- Britt, B.B., Dalla Vecchia, F.M., Chure, D.J., Engelmann, G.F., Whiting, M.F. and Scheetz, R.D. 2018. *Caelestiventus hanseni* gen. et sp. nov. extends the desert-dwelling pterosaur record back 65 million years. *Nature Ecology & Evolution*, **2**, 1386–1392, <https://doi.org/10.1038/s41559-018-0627-y>
- Butler, R.J., Brusatte, S.L., Andres, B. and Benson, R.B. 2012. How do geological sampling biases affect studies of morphological evolution in deep time? A case study of pterosaur (Reptilia: Archosauria) disparity. *Evolution: International Journal of Organic Evolution*, **66**, 147–162, <https://doi.org/10.1111/j.1558-5646.2011.01415.x>
- Butler, R.J., Benson, R.B. and Barrett, P.M. 2013. Pterosaur diversity: untangling the influence of sampling biases, Lagerstätten, and genuine biodiversity signals. *Palaeogeography, Palaeoclimatology, Palaeoecology*, **372**, 78–87, <https://doi.org/10.1016/j.palaeo.2012.08.012>
- Cheng, X., Jiang, S., Wang, X. and Kellner, A.W. 2017. New anatomical information of the wukongopterid *Kunpengopterus sinensis* Wang *et al.*, 2010 based on a new specimen. *PeerJ*, **5**, 4102, <https://doi.org/10.7717/peerj.4102>

- Close, R.A., Friedman, M., Lloyd, G.T. and Benson, R.B. 2015. Evidence for a mid-Jurassic adaptive radiation in mammals. *Current Biology*, **25**, 2137–2142, <https://doi.org/10.1016/j.cub.2015.06.047>
- Codomíu, L. and Garrido, A. 2013. New fossil record of a Jurassic pterosaur from Neuquen Basin, Vaca Muerta Formation, Argentina. *Journal of South American Earth Sciences*, **48**, 315–321, <https://doi.org/10.1016/j.jsames.2013.09.010>
- Costa, F.R. and Kellner, A.W. 2009. On two pterosaur humeri from the Azhdguru beds (Upper Jurassic, Tanzania). *Anais da Academia Brasileira de Ciências*, **81**, 813–818, <https://doi.org/10.1590/S0001-37652009000400017>
- Dalla Vecchia, F.M. 2013. Triassic pterosaurs. *Geological Society, London, Special Publications*, **379**, 119–155, <https://doi.org/10.1144/SP379.14>
- Dalla Vecchia, F.M., Wild, R., Hopf, H. and Reitner, J. 2002. A crested rhamphorhynchoid pterosaur from the Late Triassic of Austria. *Journal of Vertebrate Paleontology*, **22**, 196–199, [https://doi.org/10.1671/0272-4634\(2002\)022\[0196:ACRPFJT\]2.0.CO;2](https://doi.org/10.1671/0272-4634(2002)022[0196:ACRPFJT]2.0.CO;2)
- Dean, C.D., Mannion, P.D. and Butler, R.J. 2016. Preservation bias controls the fossil record of pterosaurs. *Palaeontology*, **59**, 225–247, <https://doi.org/10.1111/pala.12225>
- dePolo, P.E., Brusatte, S.L., Challands, T.J., Foffa, D., Ross, D.A., Wilkinson, M. and Yi, H.Y. 2018. A sauropod-dominated tracksite from Rubha nam Braithairean (Brothers' Point), Isle of Skye, Scotland. *Scottish Journal of Geology*, **54**, 1–12, <https://doi.org/10.1144/sjg2017-016>
- Fastnacht, M. 2005. The first dsungaropterid pterosaur from the Kimmeridgian of Germany and the biomechanics of pterosaur long bones. *Acta Palaeontologica Polonica*, **50**, 273–288, <https://polona.pl/preview/09590250-dc99-48dd-a895-2ed955f33840>
- Fraser, N.C. and Sues, H.D. (eds) 1997. *In the Shadow of the Dinosaurs: Early Mesozoic Tetrapods*. Cambridge University Press.
- Galton, P.M. 1980. Avian-like tibiotars of pterodactyloids (Reptilia: Pterosauria) from the Upper Jurassic of East Africa. *Paläontologische Zeitschrift*, **54**, 331–342, <https://doi.org/10.1007/BF02988135>
- Harris, J.P. and Hudson, J.D. 1980. Lithostratigraphy of the Great Estuarine Group (Middle Jurassic), Inner Hebrides, Scotland. *Scottish Journal of Geology*, **16**, 231–250, <https://doi.org/10.1144/sjg16020231>
- Hesselbo, S.P., Morgans-Bell, H.S., McElwain, J.C., Rees, P.M., Robinson, S.A. and Ross, C.E. 2003. Carbon-cycle perturbation in the Middle Jurassic and accompanying changes in the terrestrial paleoenvironment. *Journal of Geology*, **111**, 259–276, <https://doi.org/10.1086/373968>
- Hone, D.W., Tischlinger, H., Frey, E. and Röper, M. 2012. A new non-pterodactyloid pterosaur from the Late Jurassic of Southern Germany. *PLoS One*, **7**, 39312, <https://doi.org/10.1371/journal.pone.0039312>
- Hudson, J.D. and Wakefield, M.I. 2018. The Lonfean Member, Lealt Shale Formation, (Middle Jurassic) of the Inner Hebrides, Scotland. *Scottish Journal of Geology*, **54**, 87–97, <https://doi.org/10.1144/sjg2017-015>
- Jagielska, N., O'Sullivan, M. *et al.* 2022. A skeleton from the Middle Jurassic of Scotland illuminates an earlier origin of large pterosaurs. *Current Biology*, **32**, 1446–1453, <https://doi.org/10.1016/j.cub.2022.01.073>
- Jones, M.E., Benson, R.B. *et al.* 2022. Middle Jurassic fossils document an early stage in salamander evolution. *Proceedings of the National Academy of Sciences of the USA*, **119**, 2114100119, <https://doi.org/10.1073/pnas.2114100119>
- Kellner, A.W.A., Mello, A.M.S. and Ford, T. 2007. A survey of pterosaurs from Africa with the description of a new specimen from Morocco. *Paleontologia: Cenários de Vida*, 257–267.
- Korte, C., Hesselbo, S.P., Ullmann, C.V., Dietl, G., Ruhl, M., Schweigert, G. and Thibault, N. 2015. Jurassic climate mode governed by ocean gateway. *Nature Communications*, **6**, 1–7, <https://doi.org/10.1038/ncomms10015>
- Longrich, N.R., Martill, D.M. and Andres, B. 2018. Late Maastrichtian pterosaurs from North Africa and mass extinction of Pterosauria at the Cretaceous–Paleogene boundary. *PLoS biology*, **16**, 2001663, <https://doi.org/10.1371/journal.pbio.2001663>
- Lü, J. and Bo, X. 2011. A new rhamphorhynchid pterosaur (Pterosauria) from the Middle Jurassic Tiaojishan Formation of western Liaoning, China. *Acta Geologica Sinica, English Edition*, **85**, 977–983, <https://doi.org/10.1111/j.1755-6724.2011.00531.x>
- Lü, J. and Hone, D.W. 2012. A new Chinese anurognathid pterosaur and the evolution of pterosaurian tail lengths. *Acta Geologica Sinica, English Edition*, **86**, 1317–1325, <https://doi.org/10.1111/1755-6724.12002>
- Lü, J., Unwin, D.M., Jin, X., Liu, Y. and Ji, Q. 2010. Evidence for modular evolution in a long-tailed pterosaur with a pterodactyloid skull. *Proceedings of the Royal Society of London, Series B*, **277**, 383–389, <https://doi.org/10.1098/rspb.2009.1603>
- Lü *et al.* 2012 (details to be added by author).
- Martill, D.M. and Etches, S. 2012. A new monofenestratan pterosaur from the Kimmeridge Clay Formation (Kimmeridgian, Upper Jurassic) of Dorset, England. *Acta Palaeontologica Polonica*, **58**, 285–294, <https://doi.org/10.4202/app.2011.0071>
- Martin-Silverstone, E., Unwin, D.M., Cuff, A.R., Brown, E.E., Allington-Jones, L. and Barrett, P.M. 2022. A new pterosaur from Skye, Scotland and the early diversification of flying reptiles. *bioRxiv*, <https://doi.org/10.1101/2022.02.14.480264>
- O'Sullivan, M. and Martill, D.M. 2017. The taxonomy and systematics of *Parapsicephalus purdoni* (Reptilia: Pterosauria) from the Lower Jurassic Whitby Mudstone Formation, Whitby, UK. *Historical Biology*, **29**, 1009–1018, <https://doi.org/10.1080/08912963.2017.1281919>
- O'Sullivan, M. and Martill, D.M. 2018. Pterosauria of the Great Oolite Group (Bathonian, Middle Jurassic) of Oxfordshire and Gloucestershire, England. *Acta Palaeontologica Polonica*, **63**, <https://doi.org/10.4202/app.00490.2018>
- Padian, K. 1983. A functional analysis of flying and walking in pterosaurs. *Paleobiology*, **9**, 218–239, <https://doi.org/10.1017/S009483730000765X>
- Padian, K. 2008. *The Early Jurassic pterosaur Dorygnathus banthensis (Theodori, 1830) and The Early Jurassic pterosaur Campylognathoides Strand, 1928*. Special Papers in Palaeontology, **80**, John Wiley & Sons.
- Panciroli, E., Benson, R.B., Walsh, S., Butler, R.J., Castro, T.A., Jones, M.E. and Evans, S.E. 2020. Diverse vertebrate assemblage of the Kilmaluag Formation (Bathonian, Middle Jurassic) of Skye, Scotland. *Earth and Environmental Science Transactions of the Royal Society of Edinburgh*, **111**, 135–156, <https://doi.org/10.1017/S1755691020000055>
- Rauhut, O.W. and López-Arbarello, A. 2008. Archosaur evolution during the Jurassic: a southern perspective. *Revista de la Asociación Geológica Argentina*, **63**, 557–585, <http://ref.scielo.org/wj3jdb>
- Sangster, S. 2021. The osteology of *Dimorphodon macronyx*, a non-pterodactyloid pterosaur from the Lower Jurassic of Dorset, England. *Monographs of the Palaeontographical Society*, **175**, 1–48, <https://doi.org/10.1080/02693445.2021.2037868>
- Smith, R.E., Chinsamy, A., Unwin, D.M., Ibrahim, N., Zouhri, S. and Martill, D.M. 2022. Small, immature pterosaurs from the Cretaceous of Africa: implications for taphonomic bias and palaeocommunity structure in flying reptiles. *Cretaceous Research*, **130**, 105061, <https://doi.org/10.1016/j.cretres.2021.105061>
- Stecher, R. 2008. A new Triassic pterosaur from Switzerland (Central Austroalpine, Grisons), *Raeticodactylus flisurenensis* gen. et sp. nov. *Swiss Journal of Geosciences*, **101**, 185–201, <https://doi.org/10.1007/s00015-008-1252-6>
- Steel, L. 2012. The pterosaur collection at the Natural History Museum, London, UK: an overview and list of specimens, with description of recent curatorial developments. *Acta Geologica Sinica, English Edition*, **86**, 1340–1355, <https://doi.org/10.1111/1755-6724.12004>
- Steel, L. and O'Sullivan, M. 2015. A Scottish pterosaur in London: the first record of Pterosauria from the Upper Jurassic (Kimmeridgian) of Eathie (Ross and Cromarty), Scotland. *Historical Biology*, **27**, 723–728, <https://doi.org/10.1080/08912963.2014.961063>
- Sullivan, C., Wang, Y., Hone, D.W., Wang, Y., Xu, X. and Zhang, F. 2014. The vertebrates of the Jurassic Daohugou Biota of northeastern China. *Journal of Vertebrate Paleontology*, **34**, 243–280, <https://doi.org/10.1080/02724634.2013.787316>
- Upchurch, P., Andres, B., Butler, R.J. and Barrett, P.M. 2015. An analysis of pterosaurian biogeography: implications for the evolutionary history and fossil record quality of the first flying vertebrates. *Historical Biology*, **27**, 697–717, <https://doi.org/10.1080/08912963.2014.939077>
- Wellnhofer, P. 1975. Die Rhamphorhynchoidea (Pterosauria) der Oberjura-Plattenkalke Süddeutschlands I: Allgemeine Skelettmorphologie. *Palaeontographica*, **148**, 33.
- Witton, M.P. 2013. *Pterosaurs: Natural History, Evolution, Anatomy*. Princeton University Press.
- Witton, M.P. 2015. Were early pterosaurs inept terrestrial locomotors? *PeerJ*, **3**, 1018, <https://doi.org/10.7717/peerj.1018>
- Yu, Y., Zhang, C. and Xu, X. 2023. Complex macroevolution of pterosaurs. *Current Biology*, **33**, 770–779, <https://doi.org/10.1016/j.cub.2023.01.007>
- Zhou, C.F. 2014. Cranial morphology of a *Scaphognathus*-like pterosaur, *Jianchangnathus robustus*, based on a new fossil from the Tiaojishan Formation of western Liaoning, China. *Journal of Vertebrate Paleontology*, **34**, 597–605, <https://doi.org/10.1080/02724634.2013.812100>
- Zhou, C.F., Gao, K.Q., Yi, H., Xue, J., Li, Q. and Fox, R.C. 2017. Earliest filter-feeding pterosaur from the Jurassic of China and ecological evolution of Pterodactyloidea. *Royal Society Open Science*, **4**, 160672, <https://doi.org/10.1098/rsos.160672>
- Zhou, X., Pêgas, R.V. *et al.* 2021. A new darwinopteran pterosaur reveals arborealism and an opposed thumb. *Current Biology*, **31**, 2429–2436, <https://doi.org/10.1016/j.cub.2021.03.030>